Electronic Supplementary Material (ESI) for Journal of Materials Chemistry A.

Highly Stable $LiTa_2PO_8$-based Hybrid Solid Electrolytes Via In-situ Interfacial Formation Technique for Solid-State Lithium-Metal Batteries

Kumlachew Zelalem Walle[a, b, c], Yi-Shiuan Wu[a, b], Wen-Chen Chien[a, b], Masashi Kotobuki[a, b], She-Huang Wu[e], and Chun-Chen Yang[a,b,d*]

[a]Battery Research Center of Green Energy, Ming Chi University of Technology, New Taipei City 24301, Taiwan, R.O.C.

[b]Department of Chemical Engineering, Ming Chi University of Technology, New Taipei City 24301, Taiwan, R.O.C.

[c]Department of Chemistry, University of Gondar, Gondar, Ethiopia

[d]Department of Chemical and Materials Engineering & Center for Sustainability and Energy Technologies, Chang Gung University, Taoyuan City 333, Taiwan, R.O.C.

[e]Graduate Institute of Science and Technology, National Taiwan University of Science and Technology, 43, Sec. 4, Keelung Road, Taipei 106, Taiwan, R.O.C.

*Corresponding authors Tel.: +886 2 29089899 ext.4962/4952; fax: +886 2 29085941. E–mail: ccyang@mail.mcut.edu.tw (C.-C. Yang)

The Rietveld fitting analysis shows a good agreement between the observed and calculated diffraction patterns. The final R-values reached R_{wp} = 7.11% and R_p = 5.31% with a fit indicator of GOF = 3.14%.

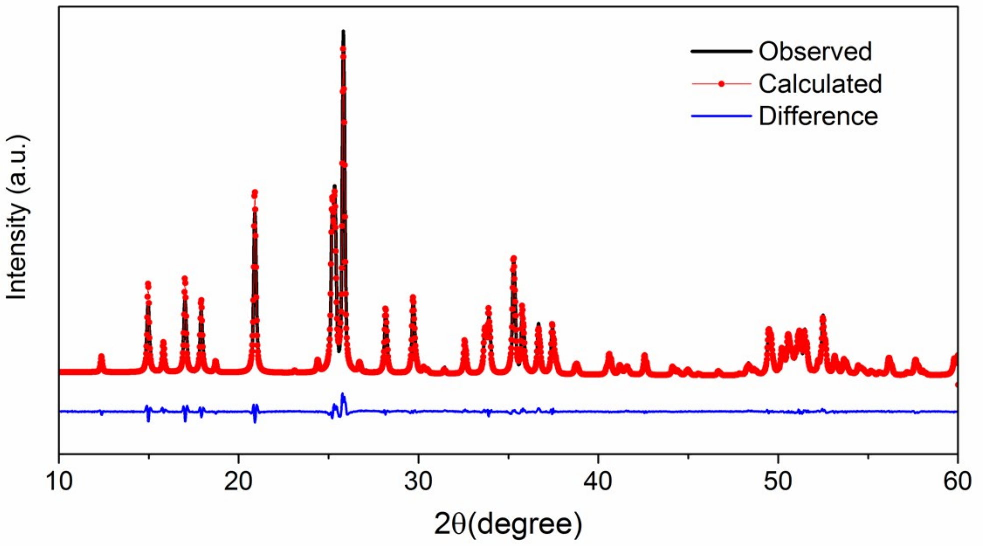

Figure S1. Rietveld refinement result of $LiTa_2PO_8$.

Table S1. Atomic parameters for $LiTa_2PO_8$.

Site	Np	x	y	z	Occ	Beq
Ta1	8	0.24561	0.09570	0.25550	1	0.3395
Ta2	4	0.00000	0.34630	0.25000	1	0.3079
Ta3	4	0.00000	0.00000	0.00000	1	0.2921
P1	8	0.49930	0.20960	0.05960	1	0.5606
O1	8	0.05690	0.33430	0.06770	1	1.224
O2	8	0.38170	0.13710	0.40610	1	1.042
O3	8	0.35820	0.50640	0.12710	1	1.271
O4	8	0.04750	0.16450	0.54970	1	1.05
O5	8	0.14430	0.23420	0.28790	1	0.8133
O6	8	0.13790	0.05670	0.11610	1	1.469
O7	8	0.37870	0.20230	0.15370	1	1.319
O8	8	0.13680	0.46550	0.28240	1	1.358
Li1	8	0.24500	0.35700	0.14000	0.72	1.658
Li2	8	0.11200	0.38700	0.40000	0.21	1.658
Li3	4	0.50000	0.00000	0.00000	0.14	1.658

Table S2. Summary of $LiTa_2PO_8$ structural information analyzed by X-ray powder diffraction.

Phase name	**Structure**
Empirical formula	$LiTa_2PO_8$
Space group	C2/c
Scale	0.00004617(77)
Cell Volume (Å^3)	1199.845(63)
Wt% - Rietveld	100.000
Crystallite Size	
Cry size Lorentzian (nm)	98.43(79)
k: 1 LVol-IB (nm)	62.66(50)
k: 0.89 LVol-FWHM (nm)	87.60(70)
Crystal Linear Absorption Coeff. (1/cm)	692.099(36)
Crystal Density (g/cm^3)	5.84371(31)
Lattice parameters	
a (Å)	9.71332(31)
b (Å)	11.53696(33)
c (Å)	10.70698(33)
β (°)	89.9079(31)

Table S3. The goodness of fit parameter

GOF	3.14
R_{exp}	2.27
R_{wp}	7.11
R_p	5.31
R_{exp}-dash	3.83
R_{wp}-dash	12.00
R_p-dash	10.73
Weighted Durbin Watson	0.39

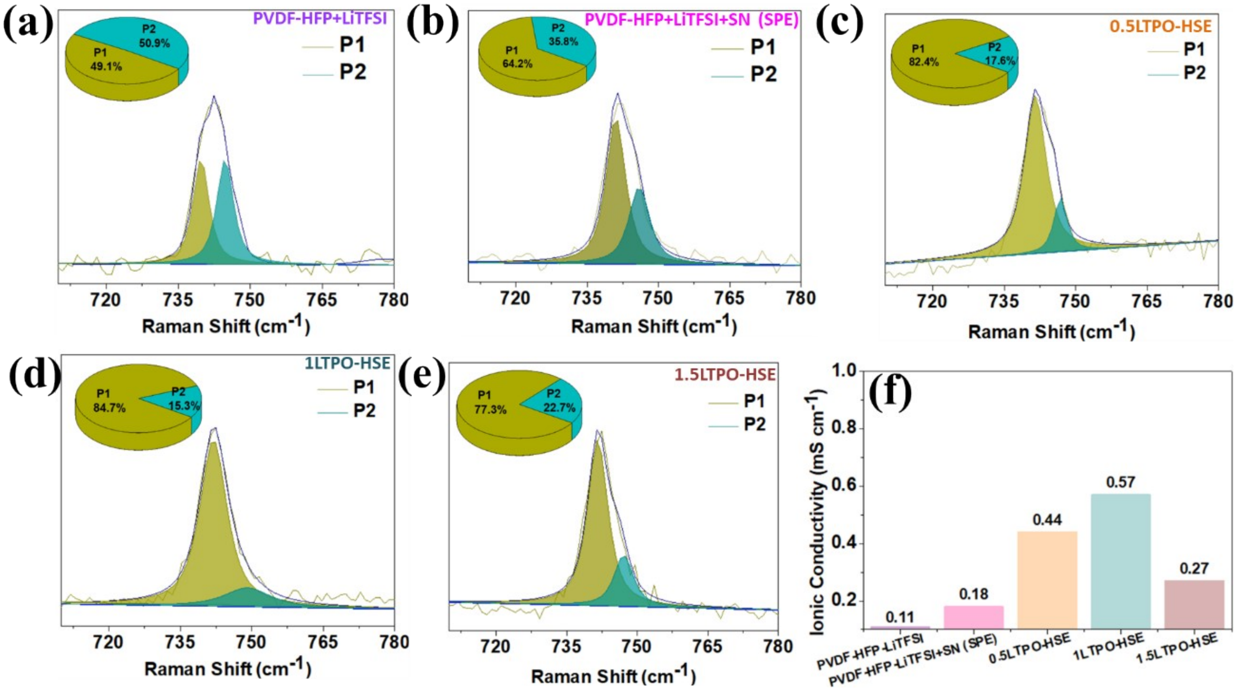

Figure S2. (a) –(e). Raman spectra and (f). Total ionic conductivity of PVDF-HFP+LiTFSI, PVDF-HFP+LiTFSI+SN (SPE), 0.5LTPO-HSE, 1LTPO-HSE, and 1.5LTPO-HSE

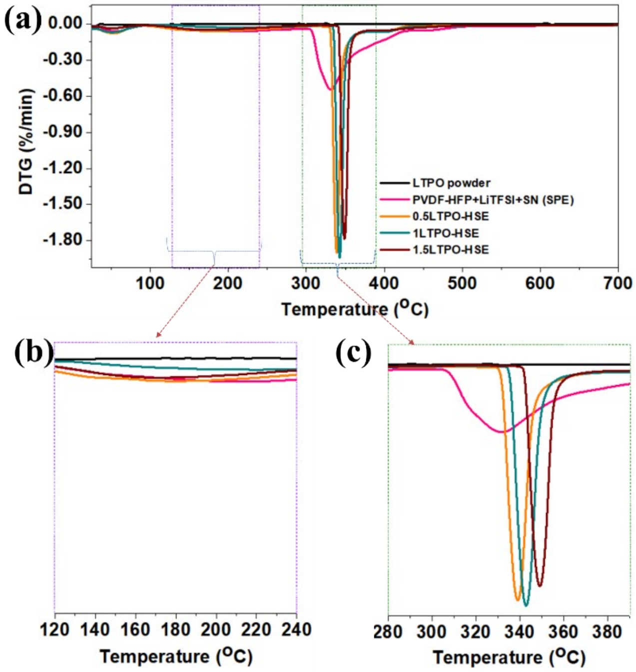

Figure S3. DTG curve of the LTPO powder and the membranes.

Particle size distribution of LTPO after 8 h ball-mill using 3D mixer. The d50 is approximately 450 µm.

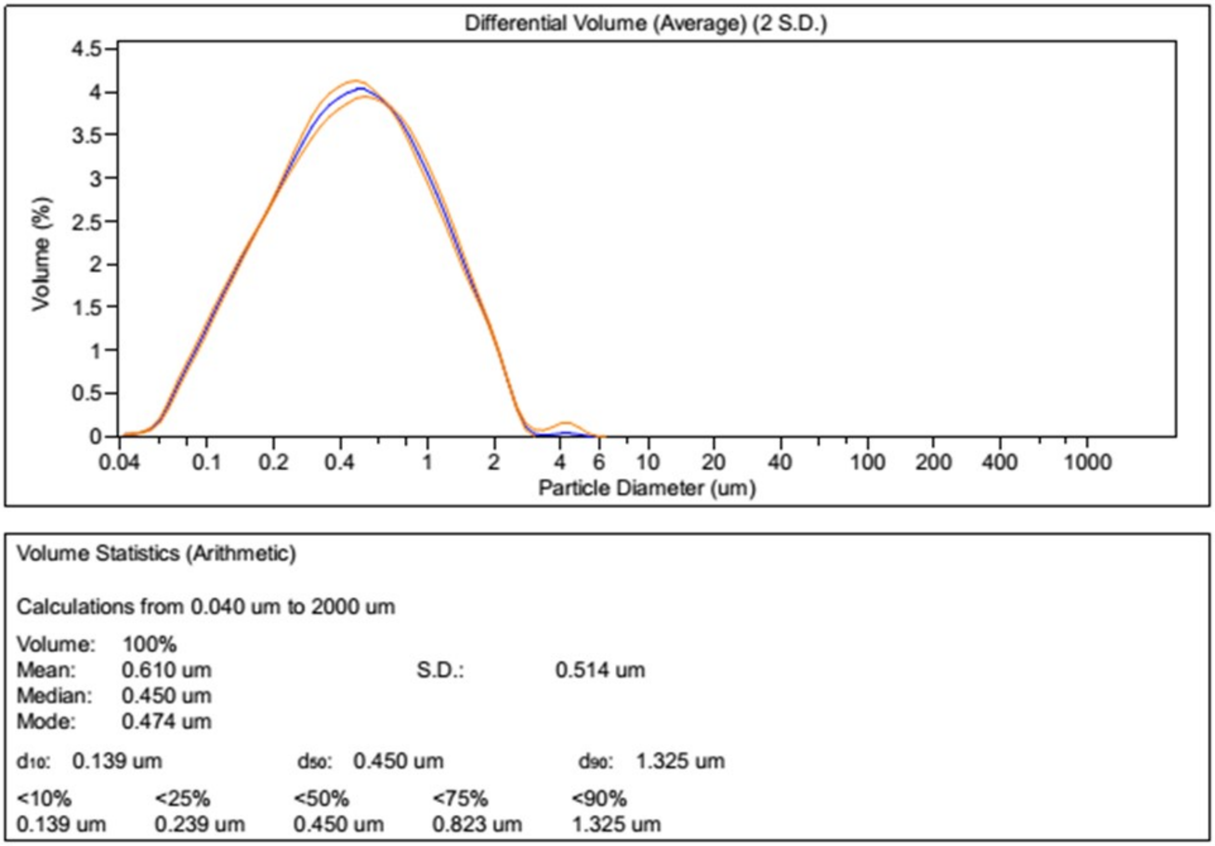

```
Volume Statistics (Arithmetic)

Calculations from 0.040 um to 2000 um

Volume:   100%
Mean:     0.610 um                  S.D.:        0.514 um
Median:   0.450 um
Mode:     0.474 um

d10:  0.139 um           d50:  0.450 um           d90:  1.325 um

<10%        <25%        <50%        <75%        <90%
0.139 um    0.239 um    0.450 um    0.823 um    1.325 um
```

Figure S4. Particle size distribution of LTPO after ball-mill using 3D mixer.

Table S4. Total ionic conductivity (σ_t in mS cm^{-1}) of LTPO pellet and 1LTPO-HSE membrane.

Temperature (^{o}C)	**LTPO pellet**	**1LTPO-HSE membrane**	**LE-1LTPO-HSE (with 10 µL) membrane**
RT	0.17	0.59	1.17
30	0.21	0.84	2.25
40	0.30	1.03	4.03

50	0.40	1.27	4.33
60	0.55	1.56	4.58
70	0.63	1.91	4.76
80	0.82	2.35	5.13

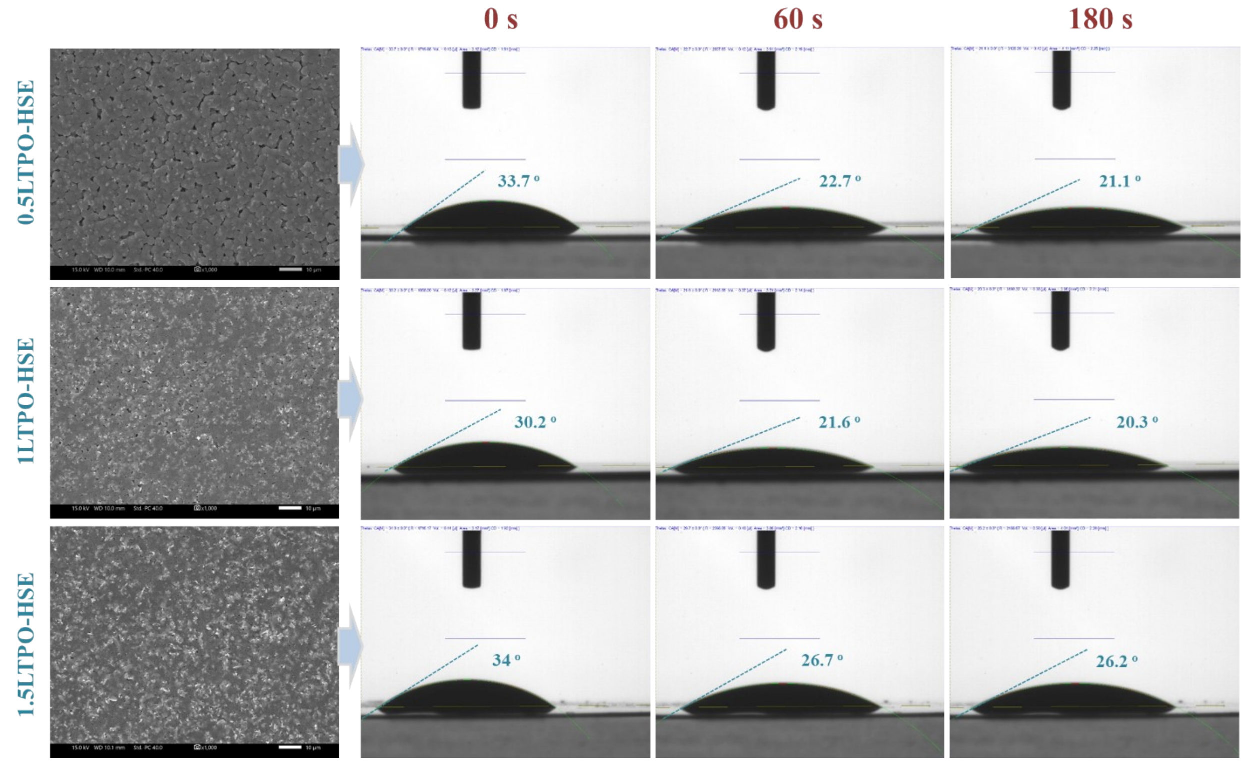

Figure S5. Contact angle measurement at 0 s, 60 s and 180 s of *x*LTPO-HSE, where x = 0.5, 1 and 1.5.

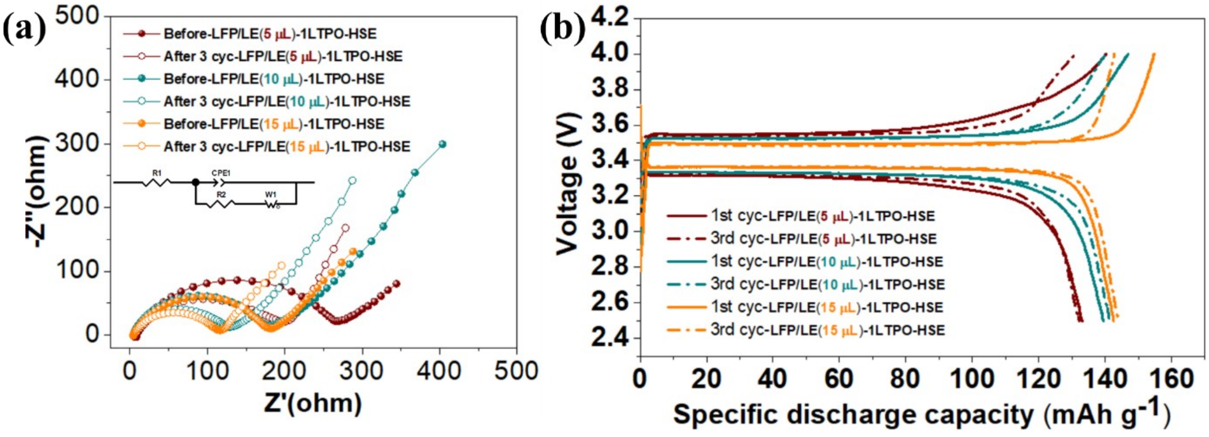

Figure S6. (a). The EIS plot of the cells before and after cycling at 0.5C for three cycles. (g) (b). The first and third charge–discharge curves of the cells with different amounts of LE additives.

Table S5. Comparison of LFP/LE(*x* μL)-1LTPO-HSE/Li cells with different amount of LE.

Sample	**Cell impedance (Ω)**				**Average coulombic efficiency (%, CE$_{avg}$)**	**Initial Specific Capacity (0.5C, mA h g^{-1})**
	R$_b$		R$_{ct}$			
	Before cycle	After 3 cycles	Before cycle	After 3 cycles		
LFP/LE(5 μL)-1LTPO-HSE/Li	6.3	8.5	265.9	202.3	97.9	133.1
LFP/LE(10 μL)-1LTPO-HSE/Li	4.1	4.7	189.2	128.7	98.4	139.6
LFP/LE(15 μL)-	4.1	4.8	183.2	114.9	97.4	142.5

1LTPO-HSE/Li

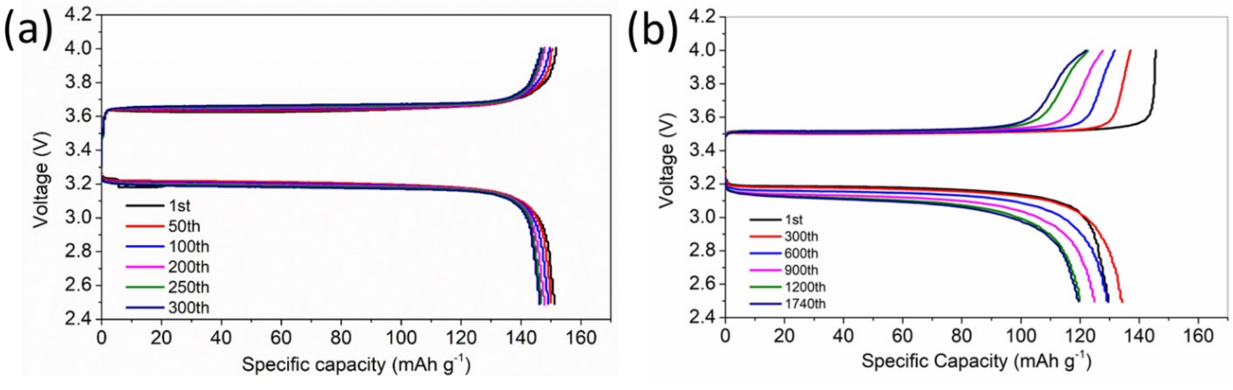

Figure S7. The voltage profile for the long-term cycling performance of (a) LFP/LE-1LTPO-HSE/Li cell with a rate of 2C/2C at 45 °C (b). LFP/LE-1LTPO-HSE/Li cell with a rate of 0.5C/2C at room temperature.

Table S6. Heat flux values for LFP/LE-1LTPO-HSE/Li and LFP/1LTPO-HSE/Li coin cells.

Operation Temperature	C rate	Heat flux (Q_t, J g^{-1}) values of cells			
		LFP/LE-1LTPO-HSE/Li		LFP/1LTPO-HSE/Li	
		Charge	Discharge	Charge	Discharge
45 °C	2C/2C	-130.0	-135.9	-126.4	-134.2
	3C/3C	-172.2	-181.6	-111.2	-123.1
55 °C	2C/2C	-103.8	-117.6	-71.9	-76.5
	3C/3C	-151.1	-163.8	-67.9	-78.8

$LiFePO_4$ composite cathode slurry was prepared to assemble a pouch cell. The same procedure was followed for the preparation step as mentioned in preparation of $LiFePO_4$ composite cathode material section. The dried composite cathode was cut to a dimension of 3.3 cm × 4.8 cm for $LiFePO_4$ cathode, 3.5 cm × 5.0 cm for Li metal anode and 3.8 cm × 5.3 cm for the LTPO-HSE in a glovebox. The active material loadings of $LiFePO_4$ in the composite cathodes for the coin cell and pouch cell were 3.5 and 4.5 mg cm^{-2}, respectively. Charge and discharge experiments were conducted on the batteries within the range of 2.5 to 4.0 V at room temperature.

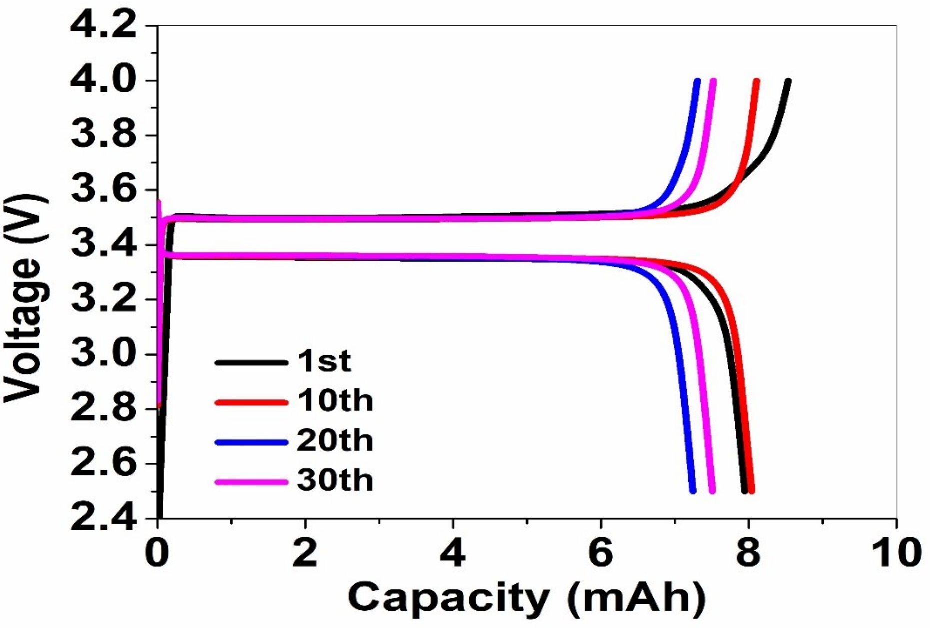

Figure S8. The voltage profile for the 3cm × 5cm LFP/LE-1LTPO-HSE/Li pouch cell with a rate of 0.1C/0.1C at room temperature,

We investigated the applicability of the LTPO-HSE membrane in the presence of LE (113 µL, based on the area of pouch cell) for pouch cell test with a dimension of 3 cm × 5 cm. One side of the carbon-coated Al foil was coated with a composite cathode material consisting of $LiFePO_4$ and assembled with Li foil (100 µm thickness) using the LE-1LTPO-HSE membrane. The pouch cell underwent cycling with a current of approximately 11 mA at a rate of 1C. The voltage curves depicted in Fig. S8, measured at 0.1C and between 2.5−4.0 V, demonstrate that the LFP/LE-

1LTPO-HSE/Li cell exhibited a capacity of 7.95 mA h (123.93 mA h g^{-1}), and even after 10 cycles, it maintained over 100% of its initial capacity at room temperature. This suggests that the use of LTPO-HSE in the presence of LE additives holds promise for applications in SSLMBs.

In the P 2p region, the peak of PO_4 in LFP cathode surface in the LFP/LE-1LTPO-HSE/Li cell is located at 133.1–133.7 eV, which is the P–O/P = O of the phosphate group in LFP and LTPO. The peak at 134.5 is also observed for the LiDFP additives. However, only two peaks for the PO_4 groups (in LFP and LTPO) are observed in LFP/1LTPO-HSE/Li cell. The presence of LiDFP additive helped for the formation of stable CEI thin film on the surface of the composite cathode material.

According to the F1s, it can be seen that there are Li-F, C-F, B-F and P-F peaks observed on the CEI layer LFP composite cathode material in the LFP/LE-1LTPO-HSE/Li cell. On the other hand, only two peaks of Li-F and C-F are observed on the LFP composite cathode surface in LFP/1LTPO-HSE/Li cell. The LiF intensity is much higher in LFP/1LTPO-HSE/Li cell than the cell with LE additive. The presence of thick LiF CEI layer on the cathode surface may diminish the diffusion of Li^+ ion which can decrease its capacity through long-term cycling. The content of LiF in LFP/LE-1LTPO-HSE/Li cell is very low, indicating the little decomposition product of the electrolyte as well as electrode components. The presence of LTPO as a catholyte (3% added during the composite cathode preparation) is also detected from the Ta 4f spectra of the CEI layer in the composite cathode material. It is shown in Fig. S9(d) that the intensity of Ta^{5+} is higher in LFP/LE-1LTPO-HSE/Li cell than without LE. This is due to the fact that, the presence of LE additives prevents the decomposition of LTPO catholyte by forming stable CEI layer on its surface.

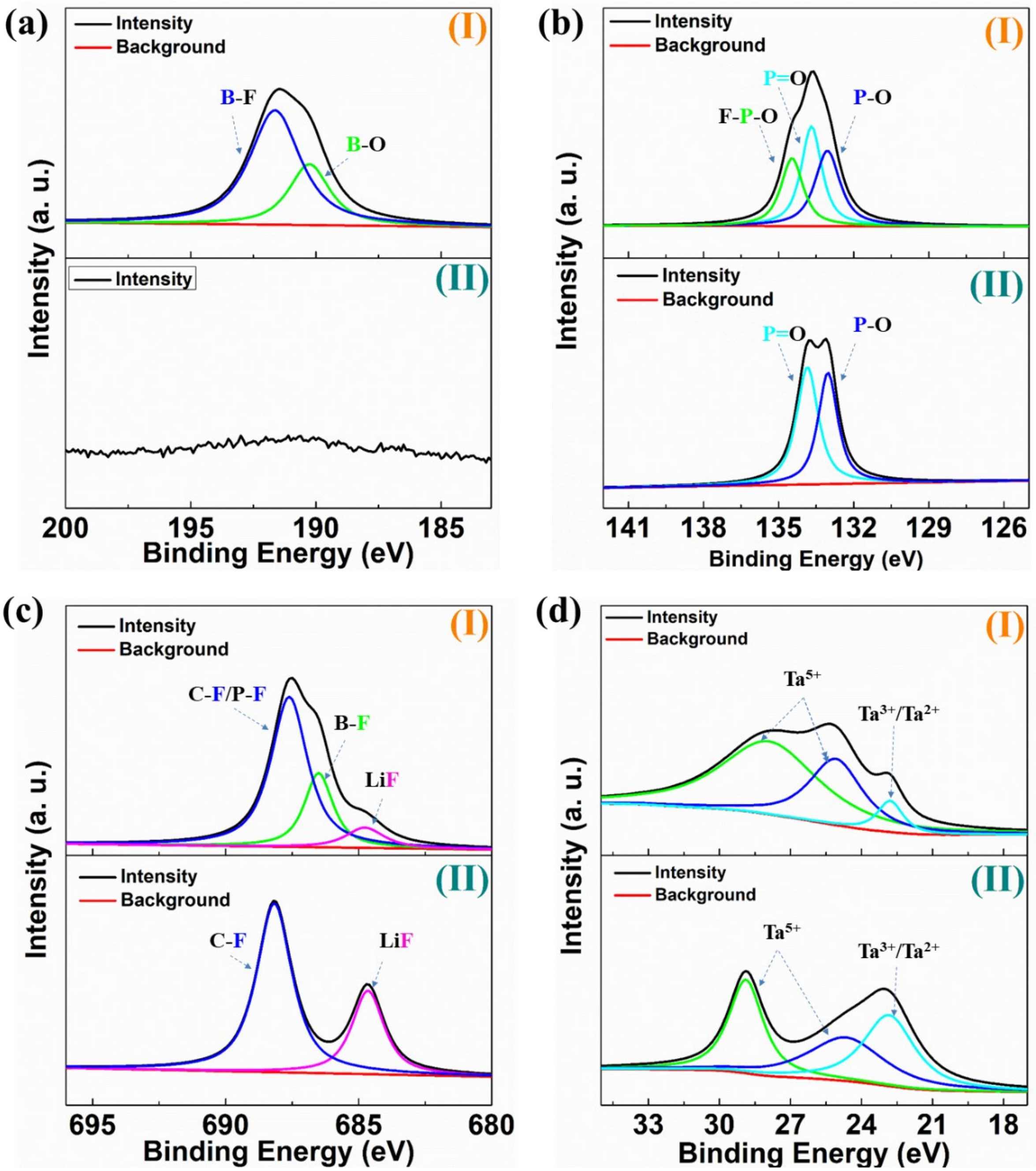

Figure S9. XPS spectra of (a). B 1s, (b). P 2p, (c). F 1s and (d). Ta 4f of the chemical composition of the surface films on the cycled $LiFePO_4$ composite cathode; (I). LFP/LE-1LTPO-HSE/Li and (II). LFP/1LTPO-HSE/Li.

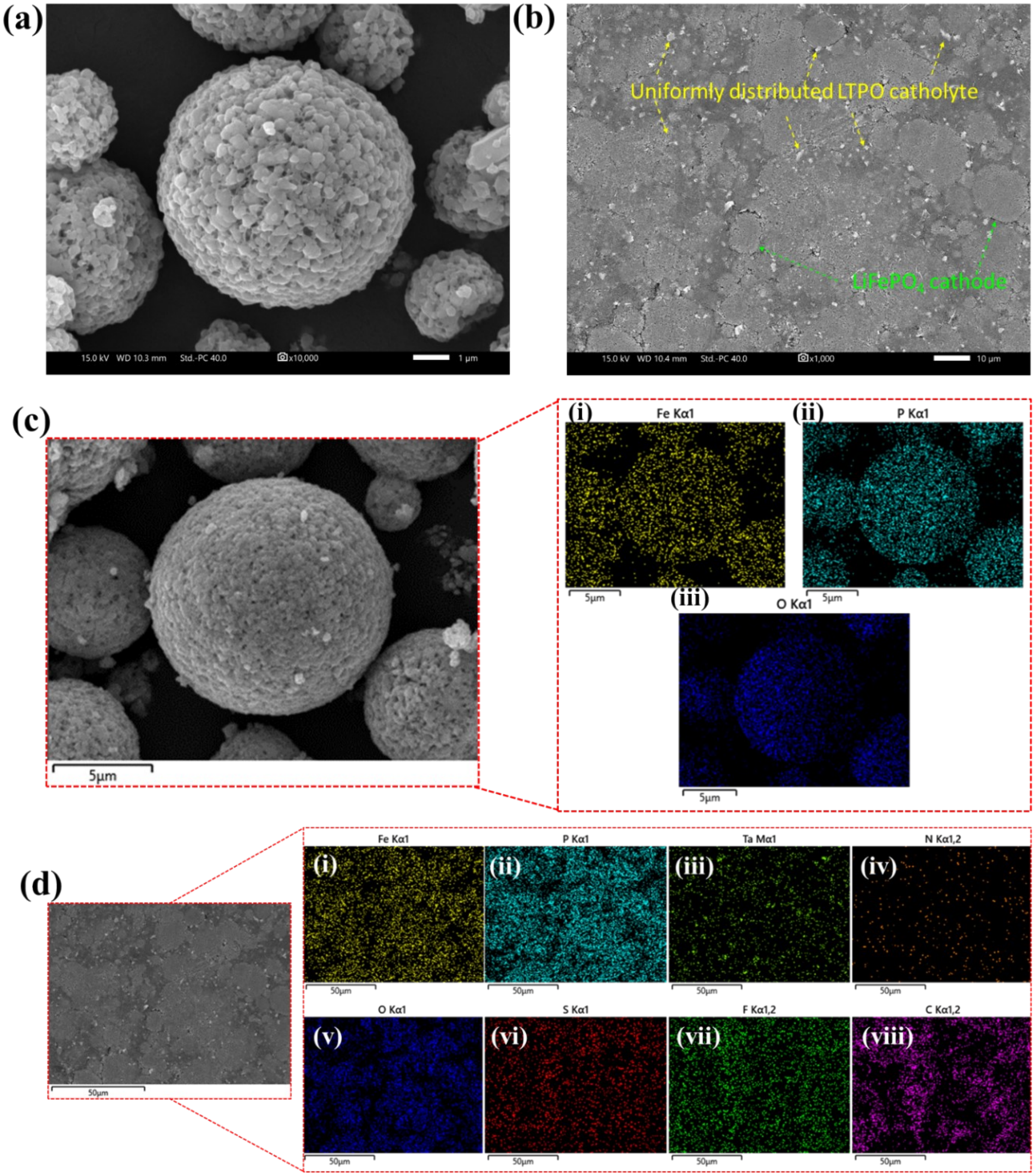

Figure S10. SEM images of (a). $LiFePO_4$ pristine powder, (b). $LiFePO_4$ composite cathode material. EDX mapping of (c). $LiFePO_4$ pristine powder, (i) Fe; (ii) P; and (iii) O. and (d). $LiFePO_4$ composite cathode material, (i). Fe, (ii). P, (iii). Ta, (iv). N, (v). O, (vi). S, (vii). F, and (viii). C.